Nematic director distribution of a liquid crystalline system presenting a cylindrical defect mode

C. BERLIC, V. BARNA[*]
Faculty of Physics, University of Bucharest, PO Box Mg-11, 077125, Bucharest, Romania

Liquid crystalline materials in complex confinement geometries have lately attracted considerable attention because of several interesting physical phenomena residing in strong surface interaction effects. Following recent investigations, we propose a Monte Carlo simulation model for characterizing the molecular director configuration in a nematic liquid crystal cell having a defect cylindrical hole in a central region of one of the boundary substrates. The main results illustrate the director's spatial profile and the local order parameter distribution for the proposed confining geometry, as well as the interaction field propagation through the bulk in the case of different anchoring regimes imposed at the boundaries.

1. Introduction

Liquid crystals (LCs) exhibit a large variety of phases and structures and, due to their particular physical properties such as fluidity, transparency, optical anisotropy, represent a convenient testing ground for many complex systems and even exotic phenomena[1-6]. Because of the large number of potential applications in the fields of science and technology [7,8] , they represent a category of very interesting materials which have drawn the attention of scientists dealing with fundamental research issues [1,2,9-11], as well as applied physical topics [1,2,4,5,12,13].

LCs are also typical examples of soft-matter systems, in which a relatively small amount of locally supplied energy may cause a response on a macroscopic scale [14]. The physical behavior of liquid crystals is largely characterized by the surface properties and, particularly, the surface anchoring energies play an important role in establishing the local orientation of the molecules. During the last decades, the interest in the study of the behavior of different condensed matter phases confined in micrometric and submicrometric cavities has increased from both fundamental and technological point of views [15]. If the confinement boundaries also present some geometric irregularities, the theoretical approach becomes very challenging, as the field orientation of the LC molecules at the interfaces and in the defect regions may assume complex configurations.

The study of the molecular arrangement in confined geometries is an important topic, not only for the correct identification of these configurations, but also for advancing in the understanding of the physical processes that occur in liquid crystalline samples.

Recently, we have observed a nonstandard behavior of electric conductivity within some samples of nematic liquid crystal (NLC) that can be associated with the local orientational order at the free surfaces of liquid crystals [16]. Different order configurations can enhance or can weaken the average overlapping of electronic clouds of neighboring molecules, modifying thus the macroscopic electric conductivity.

For better understandings on how the orientation of the local molecular director imposed by two free surfaces competes with the homeotropic alignment dictated by the electrodes of a nematic cell, Monte Carlo simulations were recently performed for a liquid crystalline system [17]. These investigations were in perfect agreement with previously obtained experimental results.

In this manuscript, we go beyond the case of an ideal system by increasing the complexity of the simulated model and characterizing the molecular director structure in a NLC sample cell presenting a cylindrical defect hole in a central region of one of the boundary substrates. The main points in our investigation are represented by the study of the director's spatial profile and the local order parameter distribution, as well as the field propagation through the bulk for different boundary anchoring regimes, in the case of the proposed confining geometry. Since the geometry of the system is rather complicated, a solution for this problem cannot be obtained by direct minimization of the free energy described by using the liquid crystal continuum theory and, eventually, Monte Carlo simulation becomes a solution of choice.

2. Molecular model and simulation method

We use the Monte Carlo simulation method as an investigation tool for the molecular order in a nematic liquid crystal cell that presents a defect located in the very center of a side boundary wall. The simulation routine is the well-known Lebwohl-Lasher model [18], which consists in a system of spins, s_i, placed in a cubic lattice, interacting with the attractive energy:

$$U_{ij} = -\varepsilon_{ij} P_2 \left(\mathbf{s_i} \cdot \mathbf{s_j} \right) \qquad (1)$$

where ε_{ij} is a positive constant (ε for nearest neighbors particles and zero otherwise) and P_2 is the second rank Legendre polynomial. This approach was widely used also in describing the properties of liquid crystal displays [19,20] and nematic structures in various confining geometries [15,17,21,22]. The main advantage of using this method with respect to other models, having also translational degrees of freedom, is the fact that spins' centers of mass are fixed, significantly reducing the computer simulation time. On the other hand, this system gives a realistic representation of a nematic liquid material, showing a first order phase transition at scaled

temperature $T_{NI}^* = \dfrac{kT_{NI}}{\varepsilon} = 1.1232$ [23].

The considered NLC system fills a cell of rectangular shape, with dimensions $L \times L \times H$ in lattice units, having the electrodes parallel with XOY plane. The bottom electrode presents a cylindrical "defect", of height H_B and radius R, as shown in figure 1. We assume periodic boundary conditions for all other directions.
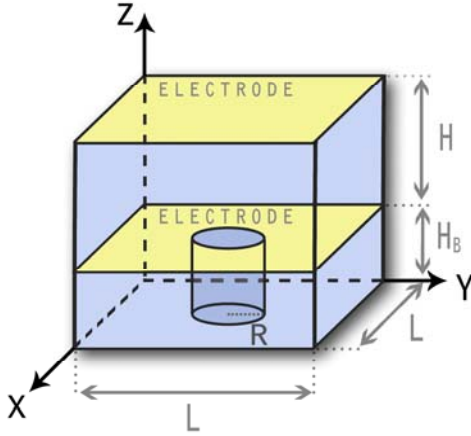

Fig. 1. Geometry for the simulated nematic liquid crystal cell, showing the cylindrical defect at one of the surfaces.

The order of the spins inside the cell is imposed by the surface boundaries. Hence, spins from layers situated in the first proximity of the electrodes are fixed and normally oriented with respect to them. On the other hand, the spins located near the wall, inside the cylindrical defect are also fixed and radialy oriented toward the main axis of the cylinder (Fig. 2). All the other spins are free to rotate.

Accordingly to this situation, we consider that the parameter ε_{ij} from equation (1) is equal to ε_B for two adjacent free moving spins and ε_S for the interaction of a free spin with a nearby fixed one. The later parameter will also describe the anchoring effects at the boundary walls [22]. At temperatures bellow T_{NI}^* a competition between these orientation tendencies is expected, resulting in an

interesting distribution of the director field inside the defect region as well as in the bulk of the simulated nematic cell.
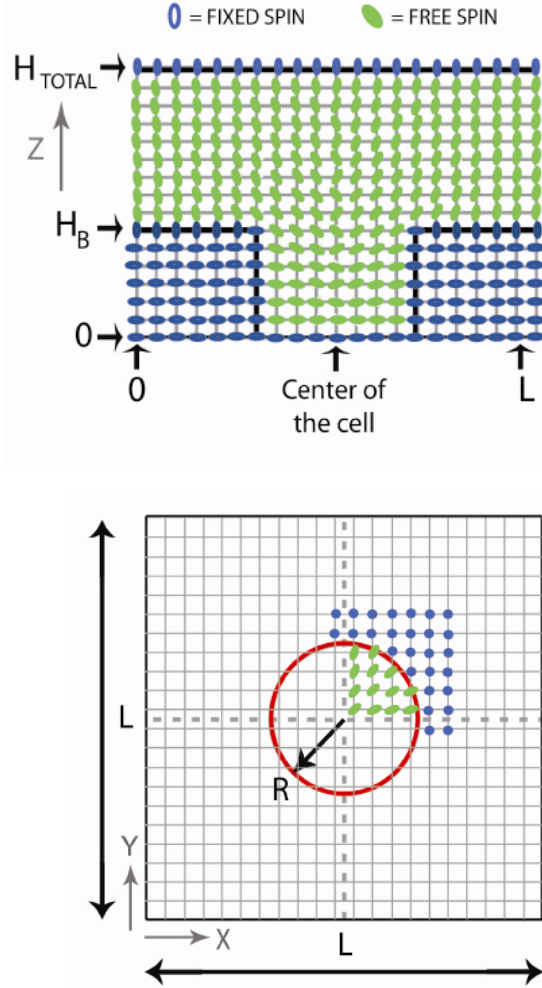

Fig. 2. Schematic for the orientation of the spins near the boundary walls of the cell. (a)Top. Cross section of the cell (parallel with the YOZ plane). (b)Bottom. Top view of the electrode presenting the defect (parallel with the XOY plane, at $z = 2$).

The order of the system is described by the local order tensor, defined as [24]:

$$Q_{\alpha\beta} = \frac{1}{n_{spin}} \sum_{k=1}^{n_{spin}} \left(\frac{3}{2} \left\langle s_{k\alpha} s_{k\beta} \right\rangle - \frac{1}{2} \delta_{\alpha\beta} \right) \qquad (2)$$

where $\alpha, \beta = x, y, z$ and $\delta_{\alpha\beta}$ is the Kronecker delta; $<...>$ is the ensemble average and n_{spin} is the number of spins. If n_{spin} is the total number of spins in the lattice, the order parameter of the bulk sample is obtained from the largest positive eigenvalue of the order tensor $Q_{\alpha\beta}$, while the corresponding eigenvector is the NLC director [25]. The biaxiality P is the absolute value of the difference

between the remaining two eigenvalues of the order tensor $Q_{\alpha\beta}$. If we choose that $n_{spin} = 1$, the average is performed on Monte Carlo cycles only and, in this case, $Q_{\alpha\beta}$ describes the local order [17]. Because of the relatively complicated geometry of the cell, we concluded that the behavior of the bulk order parameter (obtained from the Lebwohl-Lasher model) is not quite enough to describe the distribution of the nematic order. We obtained instead the simulated values of $Q_{\alpha\beta}(x, y, z)$ for all of the lattice points. With these local tensors, we found (after diagonalization) the values for the local order parameter, $S(x, y, z)$, and the director field, $\mathbf{n}(x, y, z)$, in all the points of the lattice, including the cylindrical defect region.

The Monte Carlo procedure was a standard one [24,26]: a spin was randomly picked and rotated. We calculated the energies for the old and new state and the move was allowed by using the Metropolis acceptance criterion [24,26,27]. Firstly, the system was equilibrated for 50000 Monte Carlo cycles and then we used 100000 Monte Carlo cycles for collecting the averages.

3. Results and discussion

The system described in the previous section was used to simulate the behavior of a namatic liquid crystal cell presenting a defect hole in the central region of the bottom electrode. The dimensions for the simulated box were $L \times L \times H = 34 \times 34 \times 14$ in lattice spacing units. The defect was of cylindrical shape, having radius $R = 6.5$ and height $H_B = 7$ lattice spacing, that is half of the height of the cell. It follows that the number of free rotating spins was 16540 and a Monte Carlo cycle consisted in 16540 attempted moves.
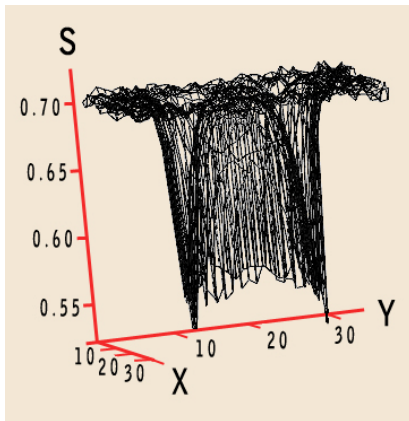

Fig. 3. Surface plot of the local order parameter in a horizontal plane situated at z=8.

We obtained the local order parameter values for all the points of the nematic cell, including the defect region, for a temperature $T^* = 0.9$, which is deep enough in the

nematic phase. By initially considering that $\varepsilon_S = 0.5\varepsilon_B$ we simulated a relatively low anchoring regime [22]. In figure 3 we plotted the obtained values for the order parameter in a horizontal plane, for $z = 8$ (i.e. near the side of the cell showing the defect). We recall that, according to figure 1, the bottom side of the cell is located in the plane $z = 7$.
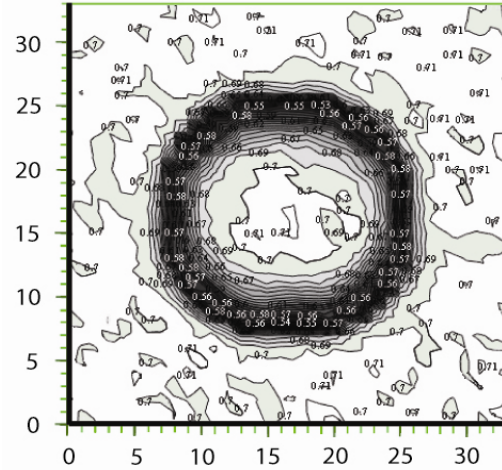

Fig. 4. Nematic order parameter for a horizontal plane situated at z=8 over the defect region. Darker areas indicate smaller values of the order parameter.

In this case, one can notice that for the regions which are not situated above the defect the order parameter is about 0.7, values which are similar to those obtained for a regular nematic cell [28]. The perspective is completely different for points positioned over the defect region. When approaching the margins of the hole, the nematic order parameter decreases to values of approximately 0.53, producing a ring-like section, as shown in figure 4. Surprisingly, it progressively increases when then advancing towards the center of the cavity, reaching a maximum value of 0.7.
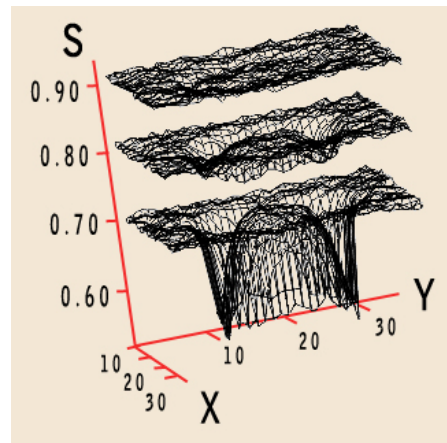

Fig. 5. Comparison between the nematic order parameter values for $z = 8$, $z = 9$ and $z = 10$. The simulated values are increased by a factor of 0.1 in this order for comprehensibility reasons.

This behavior rapidly disappears as we move further away from the defect zone, when z increases; for values $z \geq 11$ being practically unnoticeable (figure 5). This is due to the fact that the considered anchoring strength is relatively small. Other simulations were made, for the same temperature, but for strong anchoring regime ($\varepsilon_S = \varepsilon_B$), resulting in a decrease of the order parameter in the ring-like region, which persists up to $z = 13$.
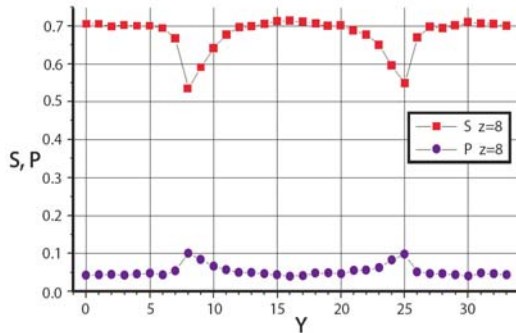

Fig. 6. Order parameter (S) and the biaxiality (P) at z=8, near the center of the cavity. Error bars sizes are of dimension of the symbols and were omitted. Lines are only guide to the eye.

This overall behavior of the order parameter lead us to the conclusion that the ring-like region where S decreases is a disclination line. For further understandings, we investigated the order parameter together with the biaxiality near the center of the cavity, that is $z = 8$ and $y = 17$ (the coordinates for the center of the cavity are $x = 16.5$, $y = 16.5$, $z = 7$, as showed in fig 1 and 2). For regions which are not near the cavity, the nematic order is uniaxial with $S = 0.7$ and $P = 0.05$, as it is expected for a homogenous bulk nematic sample. As we approach the margins of the cavity, the order parameter decreases to $S \cong 0.53$, while the biaxiality becomes $P = 0.1$; that is, the system is weakly biaxial. The order parameter and the biaxiality over the center of the cavity have the same values as for the regions that are far away from the defect. Figure 6 shows that the diameter of the ring-like disclination line is 17 lattice spacings, which is greater than the diameter of the simulated defect hole (which is 13 lattice spacings).

Inside the defect cavity, the situation is completely different. The ring-like region degenerates into two point defects, and the surface plot of S has a saddle-like shape, as it can be observed from figure 7, where we plotted the order parameter in the middle of the cavity (for $z = 4$). An important result is that the two point defects have the tendency to migrate towards the diagonal of the simulation box. We explain this behavior by admitting that between the two defects exists a repelling effect which tends to maximize the distance between them. This effect is enhanced if the initial anchoring strength is increased.
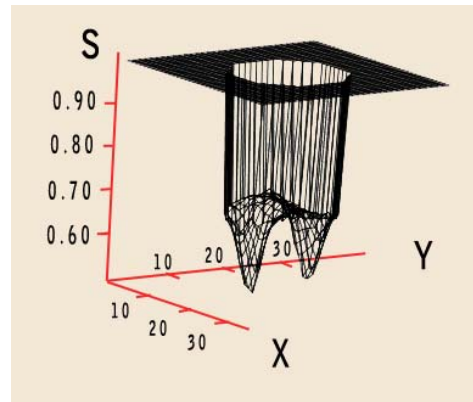

Fig. 7. Surface plot of the order parameter in a horizontal plane situated in the hole at z=4. For points having the distance from the axis of the cylinder greater than R the spins are fixed and S=1.
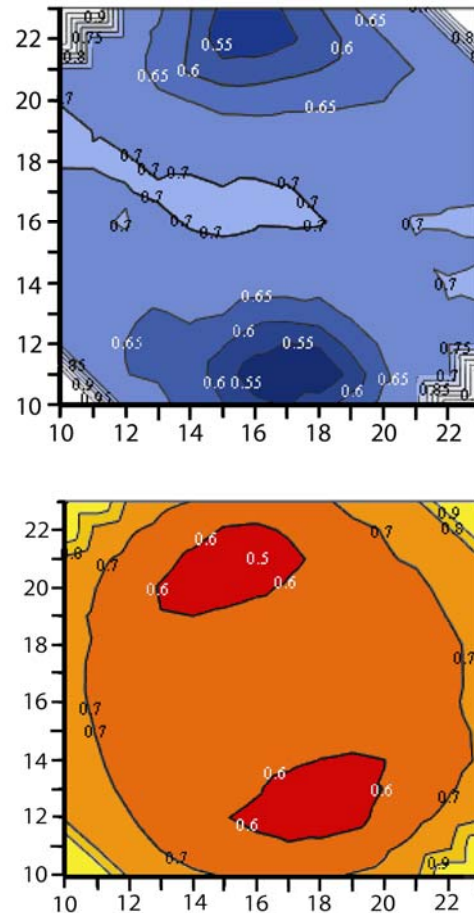

Fig. 8. (a)Top. Contour plot of the order parameter at $z = 4$ for low anchoring regime, $\varepsilon_S = 0.5\varepsilon_B$ (b)Bottom. Contour plot of the order parameter at $z = 4$ for high anchoring regime, $\varepsilon_S = \varepsilon_B$.

Fig. 8 shows what happens with the contour plots of the order parameter at $z = 4$ for low anchoring regimes, $\varepsilon_S = 0.5\varepsilon_B$, and for the higher ones, $\varepsilon_S = \varepsilon_B$.

The 'diagonalization' effect is more visible in the second situation and presents many similarities with defect structures obtained elsewhere for an elongated particle immersed in a liquid crystal host [29].

In order to elucidate the structure of these two point defects we ploted the projection of the nematic field, n, in a plane parallel with XOY plane, at $z = 4$, as it was obtained after the simulation (Fig. 9). We can conclude that near the walls of the cylinder molecules have the tendency to orient radially, but the projection of the nematic field rotates around the disclination point with a value of about 65°. However, in the disclination point, the director field is parallel with OZ axis, forming a two point "escaped structure", similar in a way with the escaped radial structure obtained for cylinders of infinite height [22].
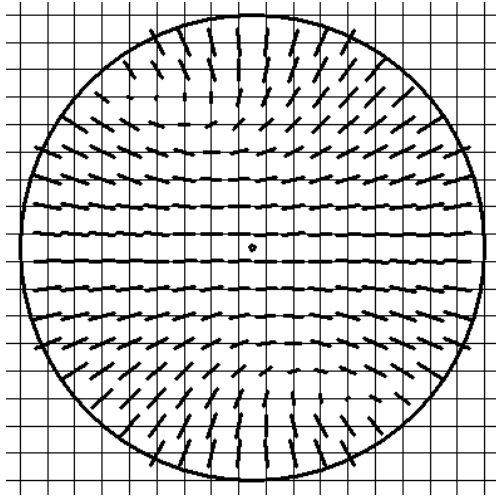
Fig. 9. Projection of the nematic director field, n, in a plane parallel with XOY, for $z = 4$ and $\varepsilon_S = 0.5\varepsilon_B$.

For nematics in cylindrical geometries, the Monte Carlo simulations and numerical stability analysis [30] showed that for a large cylinder radius and strong anchoring regime ($R\dfrac{\varepsilon_S}{\varepsilon_B} \geq 27$), an escaped radial structure should be present. In our case, we obtained an escaped radial structure even for a ratio $R\dfrac{\varepsilon_S}{\varepsilon_B} = 3.25$, and this may be explained by taking into consideration that our cylinder is short and has one bulk open cape.

In a region far away from the defect hole, the nematic configuration inside the cell should have the director parallel with OZ axis, as imposed by the boundary walls conditions. Alternatively, inside the defect region, the director tends to be radially oriented toward the center of the cylinder (i.e. normal to OZ axis), as dictated by the walls of the hole. As already demonstrated, by having to obey these two antagonistic requests, the director profile for our simulated system shows a more complicated pattern. Figure 10 pictures the contour plot of the angle between the local nematic director and OZ axis, for a plane parallel with XOZ that passes near the center of the cavity ($x = 17$), which is also intersecting the two disclination points inside the cylinder.
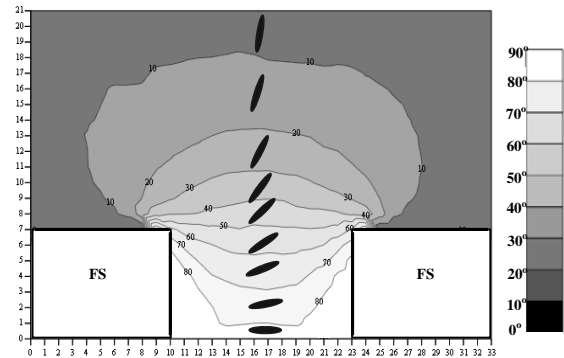
Fig. 10. Contour plot of the angle between the nematic director orientation and the OZ local axis in a plane parallel with XOZ which passes near the center of the cavity ($x = 17$); $\varepsilon_S = 0.5\varepsilon_B$. (FS – Fixed Spins).

For regions far enough from the defect hole, the nematic behaves as expected, the angle between the director and the OZ axis being up to 10°. Inside the hole, near its bottom and also in the proximity of the walls, the molecules are radialy oriented having an approximate angle of 90° with respect to the domain axis. As we go through the cap of the hole, the angle decreases, reaching a value of about 60° at its margins. The distortion of the nematic field produced by the defect hole is also propagated inside the cell, the angle becoming smaller than 10° only when $z \geq 18$. We record the general shape for the entire distortion as being similar to a "mushroom type". In the case of the strong anchoring regime, where $R\dfrac{\varepsilon_S}{\varepsilon_B} = 3.25$, the angle mapping is almost equivalent. Simulations made for $T^* = 1.3$, temperature that is above the nematic-isotropic transition, show that the molecular order inside the cell, as well as the defect cavity, disappear, even for strong boundary anchoring regimes. These results once again confirm the eligibility of our proposed simulation model.

4. Conclusions

We have used Monte Carlo simulation to investigate the local order and the competing interactions in a nematic liquid crystal cell with a defect hole at one of its boundary surfaces. Despite some limitations imposed by the relatively small dimensions of our simulated system, the

obtained results are in a good agreement with similar ones from scientific literature. By analyzing the simulated values of the local order tensor, $Q_{\alpha\beta}(x, y, z)$, we found the local order parameter values, $S(x, y, z)$, and the profile for the director field, $\mathbf{n}(x, y, z)$, in all the points of the lattice, including the cylindrical defect region. By building 2D and 3D mapping of the order parameter, we obtained a ring-like distribution around the cavity where the system is weakly biaxial. When inside the hole, the ring-like region degenerates into two repelling point defects, and the surface plot of the order parameter presents a saddle-like shape. For our simulated system, the molecular director profile inside the bulk has a relatively complicated configuration, presenting a pattern similar to a "mushroom type". Also, the results obtained for different anchoring regimes at the boundary walls and various temperatures around the nematic-isotropic transition are in good agreement with the physical phenomenological model. Our choice for the geometrical dimensions of the simulation cell assured that spins above the defect region do not directly interact with their periodical images. Consequently, we achieved an accurate mapping of the director distribution, the only influence being attributed to the defect present in the system. Yet another interesting scenario to investigate is represented by a system with a lattice of closer defects, allowing interactions between spins situated above different holes. In this situation we could simulate periodical structures such as two dimensional photonic crystals with a periodic cylindrical network filled with liquid crystalline material.

Acknowledgements

References

[1] P. G. de Gennes, J. Prost, The Physics of Liquid Crystals, Oxford Science Publications, New York (1993).

[2] L. M. Blinov, V. G. Chigrinov, Electrooptic Effects in Liquid Crystal Materials, Springer, New York (1993).

[3] V. Barna, S. Ferjani, G. Strangi, A. De Luca, C. Versace, N. Scaramazza, Appl. Phys. Lett. **87**, 221108 (2005).

[4] S. Ferjani, V. Barna, A. De Luca, C. Versace, G. Strangi, Opt. Lett. **33**(6), 557 (2008).

[5] V. Barna, R. Caputo, A. De Luca, N. Scaramuzza, G. Strangi, C. Versace, C. Umeton, R. Bartolino, G. N. Price, Opt. Exp., **14**(7), 2695 (2006).

[6] S. Ferjani, V. Barna, A. De Luca, N. Scaramuzza, C. Versace, C. Umeton, R. Bartolino, G. Strangi, Appl. Phys. Lett. **89**, 121109 (2006).

[7] V. Barna, A. De Luca, C. Rosenblatt, Nanotechnology **19**, 32 (2008).

[8] A. De Luca, V. Barna, T. Atherton, G. Carbone, M. Sousa, C. Rosenblatt, Nat. Phys. **4**, 869 (2008).

[9] A. L. Ionescu, A. Ionescu, E. S. Barna, V. Barna, N. Scaramuzza, J. Phys. Chem. B**108**(26), 8894 (2004).

[10] V. Barna, C. Miron, C. Berlic, E. S. Barna, Mater Plast, **41**(1), 15 (2004).

[11] S. Ferjani, L-V. Sorriso, V. Barna, A. De Luca, R. De Marco, G. Strangi, Phys. Rev. E **78**, 011707 (2008).

[12] A. L. Ionescu, A. Ionescu, E. S. Barna, V. Barna, N. Scaramuzza, Appl. Phys. Lett., **84**(1), 40 (2004).

[13] G. Strangi, V. Barna, R. Caputo, A. De Luca, C. Versace, N. Scaramuzza, C. Umeton, R. Bartolino, G. Price, Phys. Rev. Lett. **94**, 063903 (2005).

[14] S. Chandrasekhar, Liquid Crystals, Cambridge Monograph on Physics, Cambridge University Press (1990).

[15] G. P.Crawford, S. Zumer, Liquid Crystals in Complex Geometries, Taylor and Francis, London (1996).

[16] A. L. Alexe-Ionescu, A. Th. Ionescu, E. S. Barna, N. Scaramuzza; G. Strangi, J. Phys. Chem. B **107**, 5487 (2003).

[17] N. Scaramuzza, C. Berlic, E. S. Barna, G. Strangi, V. Barna, A. Th. Ionescu, J. Phys. Chem. B, **108**, 3207 (2004).

[18] P. A. Lebwohl, G. Lasher, Phys. Rev. A **6**, 426 (1972).

[19] E. Berggren, C. Zannoni, C. Chiccoli, P. Pasini, F. Semeria, Int. J. Mod. Phys. **6**, 135 (1995).

[20] C. Chiccoli, P. Pasini, S. Guzzetti, C. Zannoni, Mol. Cryst. Liq. Cryst., **360,** 119 (2001).

[21] C. Chiccoli, P. Passini, F. Semeria, E. Berggren, C. Zannoni, Mol. Cryst. Liq. Cryst., **290**, 237 (1996).

[22] A. M. Smondyrev, R. A. Pelcovits, Liq. Cryst., **26**, 235 (1999).

[23] U. Fabbri, C. Zannoni, Mol. Phys, **58**, 763 (1996).

[24] M. P. Allen, D. J. Tildesley, Computer Simulation of Liquids, Oxford University Press, London (1989).

[25] C. Zannoni, The Molecular Physics of Liquid Crystals, Academic Press (1979).

[26] D. Frenkel, B. Smit, Understanding Molecular Simulations. From Algorithms to Applications, Academic Press (2002).

[27] N. Metropolis, A. W. Rosenbluth; M. N. Rosenbluth, A. N. Teller, E. Teller, J. Chem. Phys. **21**, 1087 (1953).

[28] G. R. Luckhurst, P. Simpson, Mol. Phys. **47**, 251 (1982).

[29] D. Andrienko,; M.P. Allen, G. Skačej, S. Žumer, Phys. Rev. E, **65**, 041702 (2002).

[30] S. Kralj; S. Žumer, Phys. Rev. E, **51**, 366 (1995).

_____

*Corresponding author: barnavalentin@yahoo.com